Advances in Fan and Compressor Blade Flutter Analysis and Predictions

A. A. Mikolajczak,* R. A. Arnoldi,† L. E. Snyder,‡ and H. Stargardter§
Pratt & Whitney Division, United Aircraft Corporation, East Hartford, Conn.

A unified approach to flutter prediction has been developed at Pratt & Whitney Aircraft (P&WA). The aeromechanical stability of the blade-disk system is expressed in terms of a stability parameter which measures the amount of unsteady work done by the air on the system, when the system is vibrating in one of its natural modes. In neutrally stable systems, the unsteady work done by the air on the blades will balance the work dissipated by friction and by material damping. An accurate prediction of the vibrational deflections and of the unsteady aerodynamic forces is required at every spanwise location on each blade, so that the work done by the unsteady aerodynamic forces may be calculated. Recent progress is described in the prediction of unsteady aerodynamic forces and the determination of mode shapes. The stability model is applied to the prediction of supersonic flutter, chordwise bending flutter, and stall flutter. Recommendations are made for additional work necessary to improve the prediction model.

Nomenclature

A_h = aerodynamic coefficient, lift due to bending
A_α = aerodynamic coefficient, lift due to twist
A_S = aerodynamic coefficient, lift due to stiffwise
b = semichord, ft
B_h = aerodynamic coefficient, moment due to bending
B_α = aerodynamic coefficient, moment due to twist
B_S = aerodynamic coefficient, moment due to stiffwise
C_h = aerodynamic coefficient, drag due to bending
C_α = aerodynamic coefficient, drag due to twist
C_S = aerodynamic coefficient, drag due to stiffwise
D = drag, lb
h = bending displacement, ft
KE = average vibrational kinetic energy, ft-lb
L = lift, lb
M = moment, ft-lb
N = number of nodal diameters
n = number of blades
r_o = root radius, ft
r_t = tip radius, ft
s = stiffwise displacement, ft
W = total aerodynamic work, ft-lb
α = twist displacement, rad
δ = aerodynamic damping, logarithmic decrement
ρ = density, slug/ft^3
ω = circular frequency, rad/sec

I. Introduction

THE approach to flutter prediction of fans and compressors in gas turbine engines is different from the approach to flutter prediction of aircraft wings and other external aerodynamic systems. These differences arise from the greater disparity between the density of the air and the density of the structure, and from the more complex boundary to the air formed by adjacent blades and walls in the gas turbine. The density disparity makes the vibrational mode shape in the engine independent of aerodynamic effects. The complexity of the surfaces which bound the aerodynamic region, particularly the aerodynamic interaction between the cascaded airfoils, makes it virtually impossible to create aerodynamic "influence functions" which have been used successfully for aircraft flutter prediction.

In the past, the difficulties of predicting the proper unsteady aerodynamic forces for cascades of blades found in turbomachines have necessitated the use of empirical approaches to engine flutter prediction. These approaches tried to distinguish many different types of flutter and to correlate parameters measuring the onset of flutter with other structural or aerodynamic parameters. Thus, the onset of flutter was usually characterized by the relative velocity at some specified spanwise location on the blade, divided by the product of vibrational frequency and chord of the blade at that spanwise position. This was correlated against a number of parameters like the ratio of torsional to translational deflections, the relative Mach number, or the nondimensionalized incidence angle. The parametric plots served to correlate experimental data for different types of flutter, the onset of flutter being defined by an empirical boundary.

The empirical correlations have become inadequate as recent advances in technology (higher tip speeds in fans, avoidance of heavy shrouded construction, etc.) required extrapolations of past experience to new areas. The sharp dividing lines between stable operation and flutter disappeared. It became clear that the necessity for excessively conservative designs was compromising performance and that the development programs to eliminate flutter in overaggressive designs were extremely expensive. Attempts to improve the correlating parameters were unsuccessful, due to scarcity of new data and the necessity to extrapolate outside past experience. A need to develop a unified flutter prediction based on basic aerodynamics and vibration analysis, and capable of application to all new designs, became very real.

A unified approach to flutter prediction has been developed at P&WA. The aeromechanical stability of the blade-disk system is expressed in terms of a stability parameter which measures the amount of unsteady work done by the air on the system, when the system is vibrating in one of its natural modes. In neutrally stable systems, the unsteady work done by the air on the blades will balance the work dissipated by friction and by material damping. An

Received August 14, 1974. The authors wish to thank Pratt & Whitney Aircraft for their permission to publish these results. The supersonic cascade test portion of this paper was supported, in part, by the Naval Air Systems Command under Contract N00019-72-C-0187. The authors acknowledge valuable contributions to this work made by F. O. Carta and K. Stetson of the United Aircraft Research Laboratories.

Index categories: Aeroelasticity and Hydroelasticity; Subsonic and Transonic Flow; Airbreathing Engine Testing.

*Assistant Chief Engineer. Member AIAA.
†Project Engineer. Member AIAA.
‡Assistant Project Engineer. Associate Member AIAA.
§Project Engineer. Member AIAA.

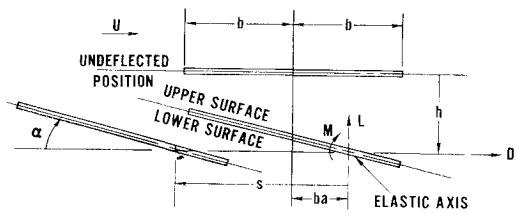

Fig. 1 Airfoil section notation showing both undeflected and deflected blade. Note: quantities positive as shown.

accurate prediction of the vibrational deflections and of the unsteady aerodynamic forces is required at every spanwise location on each blade, so that the work done by the unsteady aerodynamic forces may be calculated. This paper defines in detail the aeromechanical stability model on which a unified flutter prediction can be based. It describes the recent progress made in the prediction of unsteady aerodynamic forces and the determination of mode shapes. It then applies the stability model to the prediction of supersonic flutter, chordwise bending flutter, and stall flutter. Throughout the paper, any additional work required to improve the prediction model will be indicated.

II. Flutter Prediction Model

Flutter occurs when the unsteady aerodynamic forces and moments created by periodic blade vibrations do positive aerodynamic work on the blade during each vibration cycle and the mechanical damping is insufficient to dissipate this work input. For the purpose of flutter prediction, the results of an unsteady aerodynamic cascade analysis are expressed in terms of standard unsteady aerodynamic coefficients. Thus the time-dependent unsteady lift, drag, and moment per unit span are given by:

$$L = -\pi\rho b^3\omega^2(A_h h + A_\alpha\alpha + A_s s) \quad (1)$$

$$D = -\pi\rho b^3\omega^2(C_h h + C_\alpha\alpha + C_s s) \quad (2)$$

$$M = -\pi\rho b^4\omega^2(B_h h + B_\alpha\alpha + B_s s) \quad (3)$$

where A_h, A_α, A_s, B_h, B_α, B_s, C_h, C_α, and C_s represent the standard unsteady aerodynamic coefficients and h, s, α the instantaneous displacements as defined in Fig. 1.

The work done by the unsteady aerodynamic forces and moments on the blade in the course of the oscillatory motion of the blade is obtained by computing the product of the in-phase components of lift and vertical displacement, drag and stiffwise displacement, and moment and twist. The work done per cycle of motion in each mode is obtained by integrating the work over one cycle. The total work done on the blade per cycle of motion is given by the following expression:

$$W = \int_{r_0}^{r_t} (-\int L\cdot dh - \int D\cdot ds + \int M\cdot d\alpha)dr \quad (4)$$

where we have taken the real part of the forces and the corresponding displacements and have integrated the work per unit span over the entire span from root radius, r_o, to tip radius, r_t, to obtain the total unsteady work done on a blade.

If the rotor system (blade, disk, and shroud) is assumed to be a simple linear system, then the aerodynamic damping for the system[1] can be written as

$$\delta_{aero} = -nW/4\overline{KE} \quad (5)$$

where n is the number of blades in the rotor and KE is the average vibrational kinetic energy of the rotor system.

The total damping of the vibrating system is the sum of the aerodynamic damping and the mechanical damping. Flutter is obtained when the total damping for any vibrational mode is less than zero, i.e.,

$$\delta_{total} = \delta_{aero} + \delta_{mech} < 0 \quad (6)$$

The mode with the lowest damping is assumed to be the least stable. For flutter prediction, it is usually sufficient to examine only the lower frequency modes, namely the first three modes, since higher modes tend to have a high positive damping. Of course, it is necessary to examine the higher modes, the so-called plate-modes, using chordwise flutter predictions.

Mechanical damping consists of material damping, which can be as high as 0.02, and an unpredictable amount of frictional damping from relative motion between contacting surfaces. The aerodynamic damping can be significantly higher.

Some aircraft gas turbines operate at inlet pressures which range from a fraction of an atmosphere to several atmospheres. From Eqs. (1-6) it can be seen that aerodynamic damping is directly proportional to air density and, therefore, inlet pressure, while mechanical damping can be assumed to be virtually independent of air density. Thus, for a given amount of mechanical damping, the flutter boundary will move to earlier instability with increase in inlet pressure. This has been confirmed by tests of a supersonic fan.[2] To insure flutter free operation at all inlet pressures, the rotor system has to be designed neglecting the stabilizing effect of mechanical damping, i.e., the aerodynamic damping has to be set to be greater than or equal to zero.

Equations (4) and (5) show that the aerodynamic damping is a function of both the vibrational mode shape and the unsteady aerodynamic forces. Recent progress made in the determination of the vibrational mode shapes and in the prediction of unsteady aerodynamics will be discussed in Secs. III and IV and the application of the stability model to flutter prediction will be deferred to Secs. V and VI.

III. Determination of Mode Shapes

Mode Description

An elastic system vibrates at a unique deflection distribution for each natural frequency. A vibration of a symmetrical rotating system like a fan rotor is characterized by concentric ring nodes and traveling nodal diameters or diametral lines of zero deflection. Fig. 2 shows such a system with two ring nodes and three nodal diameters. This pattern would be referred to as a vibration in second mode with three nodal diameters. On a rotating stage the radial lines travel either forward or backward. Adjacent blades experience a relative time delay or phase difference as the wave passes; this is the "interblade phase angle" which will be shown to have a strong influence on the unsteady aerodynamic forces.

For a rotor with n blades vibrating in a N nodal diameter pattern, the interblade phase angle is $\pm(2\pi\ N/n)$ radians. For example, for a compressor rotor with 30 blades, a three-nodal diameter pattern traveling forward will set up a +36° interblade plane angle. The rotational speed of the traveling wave is related to the natural frequency of the system (ω) and is equal to $\pm\omega/N$ rad/sec. Both the

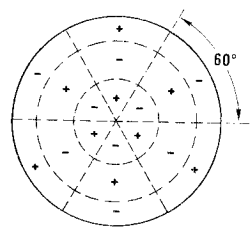

Fig. 2 Three nodal diameter pattern second mode.

forward and backward traveling waves have to be analyzed for flutter prediction to determine the least stable mode. A fan rotor consists of a set of flexible blades distributed uniformly on the periphery of a flexible rotating disk. Between the blade root attachment to the disk and the free blade tips, the blades may be joined to one another by contacting part-span shrouds. In this complex system, the torsional, the bending and the stiffwise displacements occur simultaneously but are not necessarily in phase. Therefore, it is essential to predict accurately the phase difference between the displacements if we are to predict accurately the unsteady vibrational work and the aerodynamic damping. The coupling between the torsional and bending displacements is particularly strong when either the disk is relatively flexible or there is a part-span shroud on the blades.

Vibrational Analysis

A vibration analysis has to be able to predict accurately the frequency of all the modes with all nodal diameters, and also the relative amplitudes and phases of the displacements in each mode. In the existing analysis, the disk is assumed to have the dynamic characteristics of a plate stiffened by concentric rings. Blades are assumed to act as beams and the shroud is assumed to respond dynamically like a ring. At the blade roots, local corrections for three-dimensional effects are introduced. Displacements in each mode are assumed to be distributed sinusoidally around the circumference of the stage with the number of waves equal to the number of nodal diameters. Dynamic influence equations for each section of the blading are derived and solved in finite difference form. The analysis has been quite accurate for natural frequency predictions of low order modes in current fans. For low aspect ratio fans with relatively thin blades, more sophisticated shell analyses and NASTRAN finite element analysis are being developed.

Experimental Verification of Mode Shapes

The accuracy of the analytical procedures is strongly dependent on the boundary conditions assumed at the part-span shrouds and the blade disk attachments, as well as the basic assumptions made in the analysis. Very little experimental data is available to check the mode shapes of rotating fan stages. Designers have had to content themselves with a check on the predicted resonant frequencies of the various modes using strain gages. Figure 3 describes the resonant frequencies for the first two modes of a typical shrouded fan stage and compares predictions to test data. The first-mode frequency is usually predicted with sufficient accuracy for flutter predictions. The second-mode frequency is accurately predicted at low nodal diameter modes where blade-alone response governs

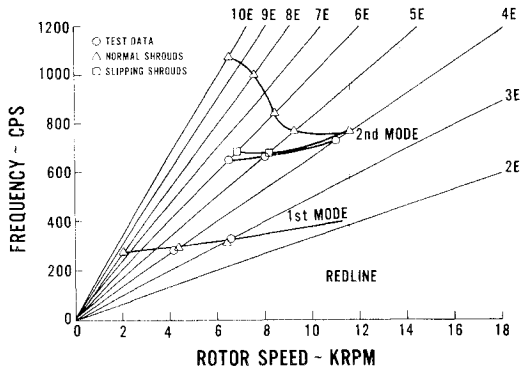

Fig. 3 Shrouded fan frequency diagram.

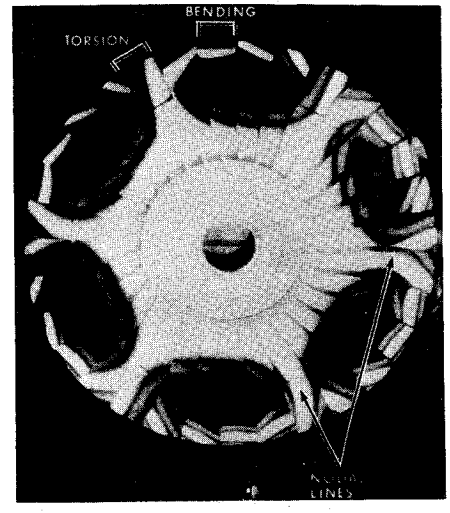

Fig. 4 Holographic measurement of vibration pattern in a bladed disk.

the stage vibration, and at high nodal diameter modes where disk and shroud effects are strong. However, some difficulty has been found in predicting the frequency at intermediate nodal diameter modes where the blade-disk-shroud interactions are significant. The disagreement is attributed to the uncertainty of the shroud boundary conditions. If we assume the shrouds to behave as partially interrupted rings which are permitted to slip, the agreement between analytical predictions and data is improved.

Even a precise prediction of natural frequencies of shrouded fan stages does not assure an accurate description of the mode shapes. A direct measurement of blade motion in flutter is necessary to verify the mode shape analysis and assure an accurate description of the deflection and twist distribution necessary for stability analysis. Successful measurements of mode shapes have been made in stationary rotors using optical techniques. Figure 4 shows a fan blade and disk assembly with part-span shrouds cemented rigidly together, vibrating in a second mode with three nodal diameters. Holography was used to produce an interferogram with nodal lines showing as bright areas and interference fringes showing the vibrational amplitude of adjacent areas. The blade tips at the nodal lines show substantial torsional motion while those halfway between nodes are primarily in translation. The mode, as pictured, is a stationary resonant mode equivalent to the superposition of two counter-rotating waves. Axial, out of plane, deflection of one blade is plotted against radial location along a blade and compared to analytical predictions in Fig. 5. Although the agreement between analysis and predictions is relatively good, the small discrepancy in the location of the node near the

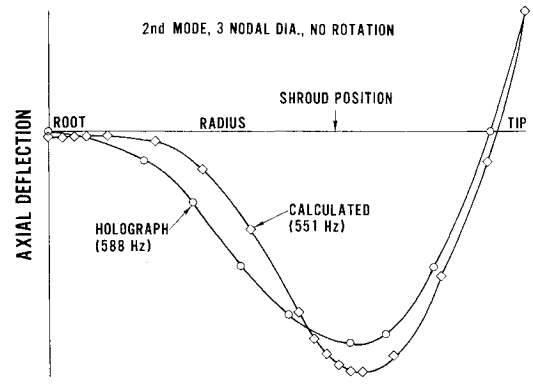

Fig. 5 Mode shape comparison—shrouded fan stage.

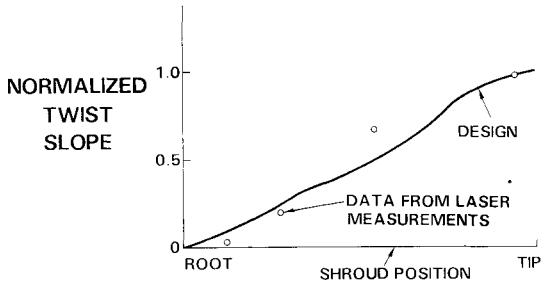

Fig. 6 Mode shape measurement in stalled flutter.

blade tip can lead to significant errors in the predicted flutter boundaries. Improvements in the mode shape analysis are now concerned with these second order effects which are related mostly to coupling between bending and torsion and the shroud boundary conditions.

Holographic measurements on static disk assemblies have advanced our understanding of the mode shapes. However, the shroud contact forces of adjacent blades are impossible to apply on full stage static tests and predictions have to be verified in rotating rigs. Although strain gages have been used extensively to determine stress distributions on rotating blades in flutter, there has been little success in translating the stress distributions in amplitudes of different components of deflections and phases between them.

The feasibility of obtaining fan mode shapes under actual operating conditions has been successfully demonstrated using reflections of laser beams from small mirrors mounted at different spanwise locations on fan blades.[3] During steady operation, the reflected light beam from each mirror returned to an identical spot on a display screen for every revolution of the rotor. However, when the blades were fluttering, the reflected beam moved from its stationary position and during successive revolutions described the blade vibration motion as a Lissajous pattern. On the first test, the instrumentation recorded only the magnitude of the displacements at different radial locations. The accuracy of the measurements for twist amplitude was approximately ±.02°, i.e., 3% of the maximum twist.

Typical second mode flutter data obtained from a research fan using the mirrors technique are shown in Fig. 6, where the measured torsional deflection (twist) of a fluttering blade operating at 70% speed is compared to the corresponding analytical predictions. Reasonable agreement between prediction and data was obtained. Current vibration analyses appear to be reasonably accurate; however, further refinements are still necessary. Optical techniques for mode shape determination, which can distinguish the magnitudes of the displacements and phase angles between bending and torsion, need to be pursued to provide guidance for future refinements in vibrational mode predictions. Such measurements can now be made with available recording systems.

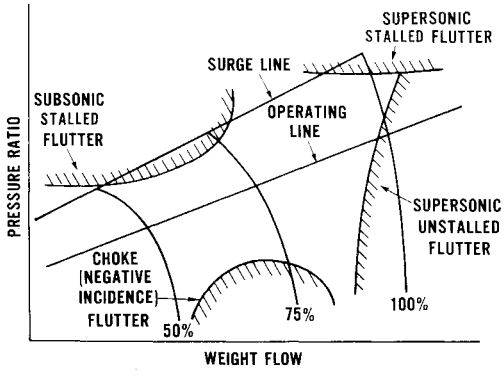

Fig. 7 Compressor map showing boundaries for four types of flutter.

IV. Unsteady Aerodynamics: Unsteady Force and Moment Prediction

Boundaries for the most common types of flutter are shown schematically on a compressor map in Fig. 7. The distinguishing features of each type of flutter and the unsteady aerodynamics relevant to flutter prediction of each type of flutter are summarized as follows.

1) *Supersonic unstalled flutter:* This type of flutter occurs when the outer span of the blade is operating supersonically and can occur at the design point or at either higher or lower pressure ratios. Its occurrence imposes a limit on high speed operation.

2) *Subsonic stalled flutter:* this type of compressor flutter is encountered near the surge line. In a high-speed fan stage, subsonic stalled flutter may occur at part-speed; in a low- or high-pressure compressor, subsonic stalled flutter may occur at or near design speed. It is suspected that during stalled flutter, separated flow may exist on the compressor blades.

3) *Choke (negative incidence) flutter:* this type of compressor flutter may occur when a fan is operating either subsonically or transonically. The stresses will increase as pressure ratio is lowered. During choke flutter, the rotor is operating at near-choke conditions and the flow is transonic over most of the blade chord.

4) *Supersonic stalled flutter:* this type of compressor flutter occurs when the outer portion of the blade is operating supersonically, and the stage is operating near the surge line. The flow has strong shocks in the blade passages.

Stalled flutter and supersonic unstalled flutter are the two most common types of flutter. In this Section, the unsteady aerodynamic analyses that are available to treat unstalled and stalled flutter will be described.

A. Unstalled Supersonic Cascade Analysis for Flat Plate Airfoils at Zero Incidence

An unsteady supersonic cascade analysis[4] applicable to supersonic unstalled flutter prediction of high speed fans has been developed. The analysis solves the "subsonic leading edge locus" problem in which the flowfield corresponds to a subsonic axial flow and a supersonic relative flow in a compressor. It accounts for the effects of inlet relative Mach number, reduced frequency, cascade geometry, pitching axis location, and interblade phase angle when calculating the unsteady pressure distribution, unsteady force and unsteady moment of a finite cascade of flat plate airfoils in a uniform supersonic inlet flowfield.

The results presented in Fig. 8 show the effect of interblade phase angle on the unsteady work for a pure pitching motion of a cascade of airfoils typical of one section of

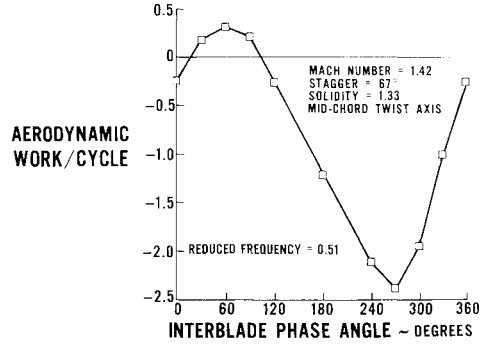

Fig. 8 Effect of interblade phase angle on unsteady aerodynamic work/cycle.

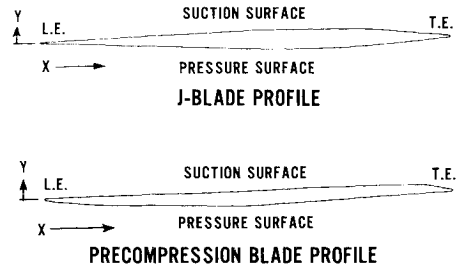

Fig. 9 Two supersonic blade sections tested.

a supersonic rotor blade. It is seen that the system is unstable for all interblade phase angles between approximately 20° and 100°, and that the least stable angle is 60°. The results emphasize the strong influence on the interblade phase angle on the magnitude of the unsteady work and hence on the onset of flutter.

In the unsteady analysis, we approximate fan blades by flat plate airfoils. To check the validity of this assumption, the influence of blade shape on flutter onset was examined experimentally by flutter testing two sets of supersonic blades in a cascade wind tunnel.[5] Two airfoil contours (Fig. 9) were evaluated; the J-blade was uncambered, symmetrical and had a 5% thickness to chord ratio. The precompression blade had a 4% thickness to chord ratio. At the design point, the J-blade had a normal shock at the passage entrance followed by subsonic flow in the passage, whereas the precompression blade had a weak shock system at the entrance and throughout the passage. The results of the supersonic cascade flutter tests are presented in Fig. 10 in the form of reduced velocity [inlet flow velocity/flutter frequency x semichord] vs. Mach number. The curves represent the incipient flutter boundary, with the unstable regions above the curves. The influence of Mach number on the flutter boundary was similar for both sets of blades. The importance of the blade shape can be assessed from Fig. 10. For a constant circular frequency (ω) and blade semichord (b) the change in the inlet Mach number at which flutter will occur is given by the intersection of a line through the origin with a slope of $a/b\omega$ where a is the sound speed. The blade shape change corresponds to approximately a 5% difference in Mach number at the onset of flutter. Since the inlet Mach number is approximately proportional to the rotor speed, neglecting the influence of blade shape can lead to a 5% uncertainty in the prediction of rotor flutter speed.

B. Unsteady Unstalled Compressible Cascade Analysis for Flat-Plate Airfoils at Zero Incidence

For some rotors, significant vibrational amplitudes can occur at spanwise locations where the relative inlet Mach number is less than 0.9. For unstalled flutter prediction of such rotors, an analysis like that developed by Smith[6] has to be used at the appropriate spanwise locations. The

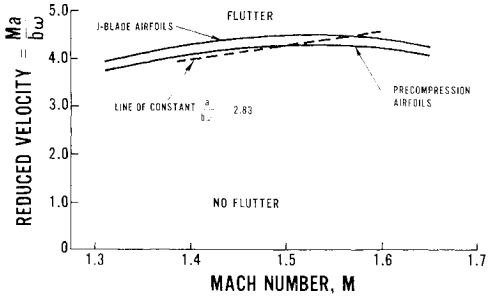

Fig. 10 Airfoil shape has minor influence on rotor flutter speed.

Smith analysis models the unsteady subsonic compressible flow through a cascade of zero thickness, zero camber airfoils at zero mean angle of attack. Application of this analysis to flutter predictions has shown that compressibility (increasing Mach number from zero) has a strong stabilizing effect on torsional modes and a small effect on bending modes.

C. Unstalled Cascade Analysis with Cambered Airfoils At Finite Incidence

There are two analyses available at P&WA which can be used to treat the unstalled, unsteady flow over a cascade of vibrating cambered airfoils. The first[7] is an extension of the flat plate analysis developed by Whitehead.[8] In this analysis, finite mean incidence and camber are accounted for; however, the analysis is restricted to incompressible flow and zero thickness airfoils. The second cambered airfoil analysis was developed by Sisto and Ni.[9] The time marching technique of solving transient flow problems was applied to the periodic unsteady flow problem. The analysis has the capability of solving for the subsonic compressible or supersonic flow through a cascade of vibrating, thick, cambered airfoils. This recently developed analysis is being used to check the effect of thickness and high camber on subsonic and supersonic unstalled flutter in fans and compressor rotors.

D. Stalled (Separated) Analysis

The area of unsteady aerodynamic analysis where boundary layer separation is important to the unsteady forces and moments is not nearly as developed as the area of unstalled, unsteady analysis. At present, only isolated airfoil analyses are available. Woods[10] developed an analysis to calculate the unsteady pressure distribution on a thin airfoil performing small harmonic oscillations in an incompressible fluid with flow separation from a prescribed stationary point on the upper airfoil surface. On the whole, it is found that a fully stalled or partially stalled airfoil has less damping than an unstalled airfoil. Sisto and Perumal[11] extended this analysis to allow for a prescribed motion of the separation point. The separation point motion is specified by a harmonic oscillation about a fixed point and a phase angle between the blade motion and the separation point motion. Additional analytical and experimental research towards the prediction of aerodynamic forces on blades operating in stalled separated flow is required.

V. Flutter Predictions

The flutter prediction model presented in Sec. II is a general model which can be applied to either unstalled or stalled flutter. The only requirements are that the flutter occur in a natural vibratory mode and that the unsteady aerodynamic forces due to small translational, and torsional motions are known. As discussed in Secs. III and IV, vibrational analyses exist to predict the possible vibrational modes in which a rotor may flutter and unsteady aerodynamic conditions. In this Section, the flutter prediction model will be evaluated against supersonic unstalled flutter data from fan rotors and its application to chordwise flutter and to subsonic stalled flutter will be discussed.

Supersonic Unstalled Flutter

Supersonic unstalled flutter is defined as the self-excited vibration of the blades in a rotor when the rotor inlet flow relative to the blades is supersonic over a significant portion of the blade span and the internal passage flow is unstalled. This flutter exhibits the following characteristics:

1) The boundary is a limit on high-speed operation as shown in Fig. 7.

2) Supersonic unstalled flutter is not related to an off-design aerodynamic condition but can occur at the design point.

3) Strain-gage records show that prior to flutter each blade in a rotor may be vibrating at a low stress level at its own natural frequency, but when flutter is encountered and the stress level becomes significant, all blades flutter at the same frequency with a constant interblade phase angle between the blades. Thus, there is a traveling wave which rotates with respect to the rotor.

4) The onset of the flutter is characterized by a sudden increase in blade stress at a natural mode frequency. It has been observed that the stress boundary is very steep; however, because of mechanical damping and non-linearities in the system, it is possible to obtain some data during flutter.

5) Flutter stress is reduced as the fan pressure ratio is increased at a constant speed. Hence, the most critical requirement is to predict the onset of flutter at the low pressure ratios.

The unsteady aerodynamic forces calculated using the linearized supersonic and compressible subsonic analysis discussed in Sec. IVA and B can be used for the prediction of the unstalled supersonic flutter boundary for high speed fans with part-span shrouds. Vibrational mode shape calculations show that for such fans only the outer 50 to 60% of the blade contributes significantly to the unsteady aerodynamic work. This is the portion of the rotor blade where the relative inlet flow is supersonic, blade camber is low, blades are thin, and at low pressure ratio the steady state shocks are weak.

The supersonic unsteady analysis and a coupled blade-disk-shroud vibration analysis have been used successfully to calculate the aerodynamic damping and hence the susceptibility to flutter of high tip speed fan rotors. Detailed comparison of predictions with experimental data will be given for two fan rotors (Rotors A and B) and then an overall comparison will be made for four additional rotors.

Rotor A was designed to experience supersonic unstalled flutter in the second mode when the relative inlet Mach number was greater than 1.4. Rotor B was an 1800 fps tip speed NASA fan stage which was designed to be flutter free. The aerodynamic damping of both rotors was calculated using Eqs. (4) and (5); spanwise integration in Eq. (4) was carried out over the portion of the blade where the relative inlet Mach number was greater than 1.1. For both rotors, the first three vibrational modes were analyzed to identify the least stable mode.

Rotor A

The rotor design is summarized in Table 1. The blade aspect ratio, part-span shroud location and thickness distribution were chosen so that unstalled supersonic flutter would occur in the second mode. The rotor experienced supersonic unstalled flutter at 13,290 rpm while accelerating along a low pressure ratio operating line. Flutter occurred in the second mode with a four-nodal diameter vibrational pattern.

Table 1 Design parameters

	Rotor A	Rotor B
Tip Speed	1800 fps @ 15,000 rpm	1800 fps @ 12,464 rpm
Hub to tip ratio	0.38	0.50
Aspect ratio based on root chord	4.00	2.87
Part-span shroud position	50%	65%

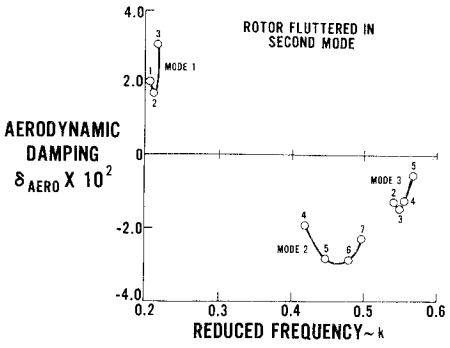

Fig. 11 Damping predictions for P&WA research rotor at flutter speed.

The predicted aerodynamic damping for the least stable nodal diameters of the first three vibrational modes of the rotor is given in Fig. 11. The calculated values show that, for low pressure ratio operation at this rotor speed, the second coupled mode is the least stable mode. The aerodynamic damping of the least stable vibrational mode is negative. Since flutter occurs when the sum of the aerodynamic damping and mechanical damping equals zero, a negative value of aerodynamic damping is necessary before flutter will occur in a rotor where mechanical damping is present.

The sensitivity of aerodynamic damping to rotor speed is shown in Fig. 12. The rotor has been analyzed at three different rotor speeds, the lowest being where the least stable nodal diameter in the second mode has nearly zero aerodynamic damping. It can be seen that susceptibility of the rotor to flutter is reduced when speeds are lowered. The amount of mechanical damping in this rotor has not been measured, but estimates based on material damping alone[12] indicate that it could be as high as 0.02. At this level of damping, the predicted rotor flutter speed would be 5% lower than the actual speed at which flutter occurred. If we assume that the total mechanical damping (material damping and frictional damping at part-span shrouds and rotor root attachments) is approximately 0.03, then the predicted and the actual rotor speed at which flutter occurred match exactly. These comparisons show that the analysis predicts accurately the least stable flutter mode. However, it is conservative in predicting the rotor speed at which flutter occurs if the mechanical damping is assumed to be no greater than that due to the material hysteresis damping alone.

Rotor B

Rotor B was designed to be flutter-free; its design is also summarized in Table 1. This rotor was tested suc-

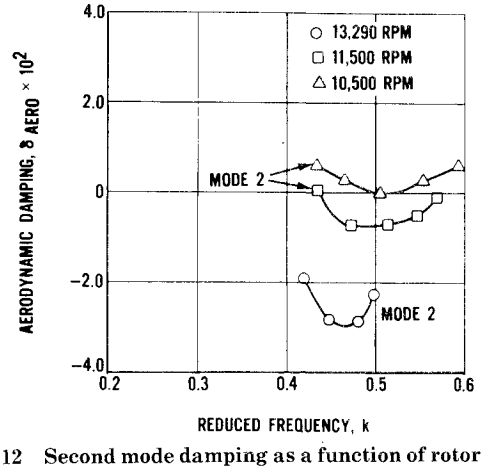

Fig. 12 Second mode damping as a function of rotor speed.

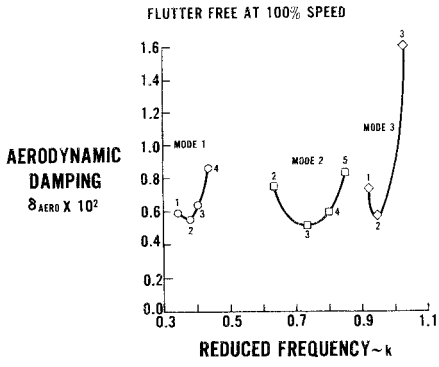

Fig. 13 Damping prediction for NASA 1800 fps rotor at 100% speed.

cessfully to 12,464 rpm[13] and no supersonic unstalled flutter was observed. Figure 13 shows the results of analyzing the rotor at the maximum speed condition. All modes are calculated to have positive aerodynamic damping at this most severe condition. It can be seen that the design is optimized insofar as all the vibrational modes exhibit the same aerodynamic damping at this rotor speed. The high positive aerodynamic damping shows this fan to have been conservatively designed.

Other Rotors

The supersonic unstalled flutter analysis has been applied to both shroudless and single and double shrouded fan stages and excellent agreement obtained between predictions and data. Figure 14 summarizes the ability of the analysis to predict correctly the relative stability between modes. It can also be seen from Fig. 14 that whenever flutter was observed, the analysis predicted a level of negative aerodynamic damping which was comparable to the expected level of mechanical damping of the rotor. Rotor 3 in Fig. 14 would be judged to be very close to flutter at its highest operating speed. The accurate flutter prediction model described in this Section which is capable of identifying the relative closeness of different natural vibrational modes to flutter, will provide engine designers with a valuable tool for optimization of rotor designs.

Chordwise Blade Flutter

For very high speed fans for which composite materials are currently being developed, supersonic unstalled flutter can occur in a vibratory mode which involves a large vibrational deformation of the blade camber line. Such modes are present and important near blade tips when the rotor aspect ratio is low and the blades are thin. The vibratory natural modes can currently be predicted using shell analysis or NASTRAN. The unstalled supersonic analysis has been extended (Ref. 14) to calculate the aerodynamic forces for typical chordwise blade deformation

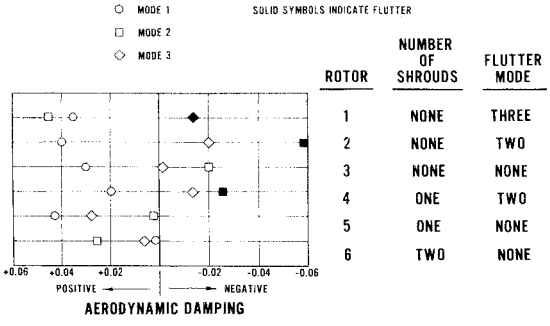

ROTOR	NUMBER OF SHROUDS	FLUTTER MODE
1	NONE	THREE
2	NONE	TWO
3	NONE	NONE
4	ONE	TWO
5	ONE	NONE
6	TWO	NONE

Fig. 14 Damping analysis as an unstalled supersonic flutter prediction tool.

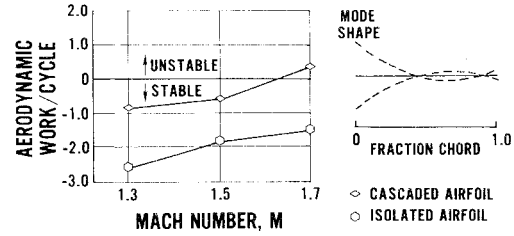

Fig. 15 High Mach number increases the possibility of chordwise bending flutter.

shown in Fig. 15. The vibrational mode shape and the unsteady aerodynamic work shown in Fig. 15 have been calculated for the fourth mode of a tip section of a 1.2 aspect ratio, high speed, shroudless blade. It can be seen that the susceptibility to flutter increases with Mach number and that although an isolated airfoil is relatively stable, the possibility of chordwise flutter in fans becomes very real at high tip Mach numbers. Experimental verification of the predictions is still required.

Stalled Flutter

Stalled flutter usually occurs near the compressor surge line, and is identified by an increase in flutter stress as pressure ratio is increased at constant speed.

There are no experimental data available to indicate whether at the onset of flutter the flow is fully attached along the blade suction surface or is separated during part of the blade oscillation or is separated during the entire blade oscillation. Time-averaged flow measurements taken recently in a research fan stage during stall flutter have shown that aerodynamic losses behind the rotor did not increase measurably as the flutter boundary was crossed. Hence, it does not appear that a large portion of the blade was stalled during flutter. Furthermore, in some instances the stall flutter boundary has been observed to occur near maximum compressor efficiency indicating that stalling is not an essential condition for "stalled" flutter, although it could be the most severe condition. The above observations indicate that the influence of flow incidence on the unsteady aerodynamic forces will have to be considered in the prediction of the flutter boundary.

An incompressible, unsteady flow analysis for small flow turning (described in Sec. IVC) was used in combination with the coupled blade-disk shroud vibrational analysis to calculate the predicted aerodynamic damping for the first three vibrational modes of a number of shrouded fan stages operating at part speed. The second mode was predicted to be the least stable. Flutter was observed to occur in the second mode in all cases. However, the aerodynamic damping in the least stable mode, although small, remained positive even when the incidence was increased past the measured values. Hence, it does not appear that an incompressible, unsteady analysis for cascades with low flow turning can be used to accurately model the unsteady flowfield present during tthe "stalled" type of flutter.

To refine the predictions and determine more accurately the effects of incidence, the unsteady aerodynamic analysis[7] has been extended to include high turning. Furthermore, the recently developed analysis[9] which treats the compressible unsteady flow past a cascade of oscillating, thick, high camber airfoils is also being evaluated against the experimental flutter data. Intuition suggests that the effects of viscosity and boundary-layer separation will have to be considered in stalled flutter predictions, particularly if we are to assess when the flutter boundary is sufficiently far removed from the compressor surge line to prevent onset of flutter during transient engine operation. At present, there are no unsteady, separated flow cascade analyses available. The closest is an analysis de-

veloped by Sisto and Perumal.[11] This analysis will have to be supplemented by empirical information on the oscillation of the flow separation point in order to become a useful flutter prediction tool.

From this discussion, it is apparent that controlled, basic experimental programs are required to verify and complement the unsteady aerodynamic predictions. Such a program is being implemented at United Aircraft using a subsonic oscillating cascade. The airfoils in the cascade will be oscillated by a single drive to insure a coherent frequency of all airfoils; a system of cams will provide the desired interblade phase angle between the airfoils. An airfoil in the cascade will be equipped with miniature differential pressure transducers and hot film transducers to measure the pressure-time history and measure transition and separation in the boundary layer during the oscillatory motion. The cascade tests will be performed at several interblade phase angles and at amplitudes of motion representative of those observed during rotor stalled flutter. The cascade tests will provide extensive and reliable data in a closely controlled environment. However, to confirm the validity of the cascade results, a rotor test will be required. An ideal vehicle would be a research fan of high performance and tip speeds typical of current advanced fan designs.

VI. Conclusions

1) A unified approach to flutter prediction has been derived which eliminates the need for extensive empirical correlations and can be used to design flutter-free rotors beyond current levels of technology. In this approach, the sum of aerodynamic damping and mechanical damping has to be greater than zero to insure flutter-free operation. Calculation of aerodynamic damping requires an accurate prediction of vibration displacements and unsteady aerodynamic forces.

2) The current prediction of vibrational displacements are relatively accurate; however, additional work is required to refine the boundary condition assumption at part-span shrouds and blade root attachments. The predictions for stationary blade disk assemblies have been verified using holographic techniques. Significant progress has been made towards measurements of deflections in rotating assemblies using optical techniques.

3) Unsteady aerodynamic forces have been accurately predicted for supersonic flow in cascades of thin, uncambered airfoils. Progress has been made towards predicting unsteady forces in compressible flow in cascades of highly cambered airfoils.

4) An accurate flutter prediction has been developed for supersonic unstalled flutter and significant progress made towards prediction of stalled flutter.

5) Aerodynamic damping has been shown to be strongly dependent on air density and to be significantly higher than mechanical damping. For engines which have to operate over a wide inlet pressure range, and therefore a wide inlet density range, it is advisable to set the aerodynamic damping to be positive over the complete compressor operating map if we are to avoid onset of flutter at high inlet pressures.

References

[1]Carta, F. O., "Coupled Blade-Disc-Shroud Flutter Instabilities in Turbojet Engine Rotors," *ASME Transactions, Journal of Engineering for Power,* Vol. 89, July 1967, pp. 419–426.

[2]Jeffers, J. D. and Meece, C. E, "F100 Fan Stall Flutter Problem Review and Solution," *Journal of Aircraft,* Vol. 13, May 1975, pp.

[3]Stargardter, H., "Optical Determination of Rotating Fan Blade Mode Shape," to be published.

[4]Verdon, J. M., "The Unsteady Aerodynamics of a Finite Supersonic Cascade with Subsonic Axial Flow," *ASME Transactions, Journal of Applied Mechanics,* Ser. E, Vol. 40, Sept. 1973, pp. 667–671.

[5]Snyder, L. E. and Commerford, G. L., "Supersonic Unstalled Flutter in Fan Rotor: Analytical and Experimental Results," ASME Paper 74-GT-40 1974.

[6]Smith, S. N., "Discrete Frequency Sound Generation in Axial Flow Turbomachines," Rept. CUED/A-Turbo/TR29, 1971, Univ. of Cambridge, Cambridge, England.

[7]Anon., "The Calculation of Aerodynamic Forces and Moments on Airfoils Vibrating in Cascade," Rept. 1084-1, prepared for Pratt & Whitney Aircraft, June 1964, Northern Research and Engineering, Cambridge, Mass.

[8]Whitehead, D. S., "Force and Moment Coefficients for Vibratory Airfoils in Cascade," R and M 3254, Feb. 1960, British Aeronautical Research Council, London.

[9]Sisto, F. and Ni, R., "Research on the Flutter of Axial Turbomachine Blading," ONR Tech. Rept. ME-RT 74-008, May 1974, Stevens Institute of Technology, Hoboken, N.J.

[10]Woods, L. C., "Aerodynamics Forces on an Oscillating Airfoil Fitted with a Spoiler," *Proceedings of the Royal Society (London)* Ser. A, Vol. 239, 1957, pp. 328–337.

[11]Sisto, F. and Perumal, P. V. K., "Lift and Moment Predictions for an Oscillating Airfoil with a Moving Separation Point," ASME Paper 74-GT-28, 1974.

[12]Lazan, B. J. and Goodman L. E., "Material and Interface Damping," Sec. 36 of Harris and Crede, *Shock and Vibration Handbook,* Vol. 2, McGraw-Hill, New York, 1961.

[13]Morris, A. L. and Sulam, D. H., "High-Loading, 1800 ft/sec Tip Speed Transonic Compressor Fan Stage-II Final Report," CR-120991, PWA-4463, Dec. 1972, NASA.

[14]Snyder, L. E., "Supersonic Chordwise Bending Flutter in Cascades," First Quarterly Tech. Rept., NASC Contract N00019-74-C-0305, Rept. PWA-5061, Aug. 1974, Naval Air Systems Command, Washington, D.C.